Head and Neck Squamous Cell Carcinoma Tumor Response to Controlled Treatment in Mouse Model

Chad Phillips[1], Dmitriy Major[2], Romina Shirazi[3], and Antonio Loaiza[4]

[1234]*Shu Chien-Gene Lay Department of Bioengineering, University of California San Diego*
(all authors contributed equally)
[1]cbphilli@ucsd.edu
[2]dmajor@ucsd.edu
[3]roshirazi@ucsd.edu
[4]aloaiza@ucsd.edu

***Abstract*— Head and Neck Squamous Cell Carcinoma (HNSCC), is a particular subtype of cancer that has been shown to have common connections between heavy smokers. In order to understand this cancer subtype better, a cell line was created that mimics the HNSCC to be tested on non-human subjects, an example of which being live mice in a controlled laboratory. This controlled setting allows for the treatment to be a controlled variable to examine the cause-effect relationship of adjusted treatment. Our team will be evaluating an established biosystem of a live mouse containing developed cancer tumors with the goal of modeling a volumetric profile and concentration profile based on the treatment drug given to the mouse samples. Immunotherapy and radiation therapy are introduced to the biosystem as control measures to model the effects of treatment. Our team will analyze a system of combination of both treatments to model improvement in the stability of the biosystem (in this case leading to a decrease in tumor volume). Based on experimental evidence as well as the modeled theoretical response, both the radiotherapy and drug treatment proved effective at reducing tumorigenesis; however, the combination of both treatment options proved to be more effective than either singular option available.**

***Keywords* — PD Control, Cancer, Head and Neck Squamous Cell Carcinoma, Frequency Response, aPD-1, Radiotherapy**

I. Introduction

A. Background

Head and Neck Squamous Carcinoma (HNSCC) is a very serious form of oral cancer commonly found in oral cavities, larynx, and pharynx, with a high incidence rate amongst heavy smokers. The cancer itself is a highly afflictive disease, affecting those diagnosed with pain, disfigurement, speech, and even vital aspects of breathing and swallowing[1]. Fortunately, despite having such a high level of impact on day-to-day lifestyle for those afflicted with the cancer, HNSCC is highly predisposed to imaging via biopsy at all stages of cancer from tumorigenesis to metastasis, resulting in a higher understanding of the cancer compared to some other subtypes[1].

While HNSCC generally has a higher diagnosis rate associated with heavy smokers, drinkers, and other forms of alcohol abuse, a couple of forms of the carcinoma–particularly those associated with pharyngeal diagnoses–are generally attributed to other factors such as Human Papilloma Virus (HPV)[2]. Despite the ability to image the cancer via biopsy, HNSCC is generally diagnosed at later stages due to the relative difficulty of non-invasive imaging of the disease. In fact, the majority of HNSCC diagnoses occur with careful physical examination as the primary approach[2]. Nonetheless, once diagnosed, the cancer is treated through a combination of surgery and chemoradiotherapy (CRT). While the combination of surgery and radiotherapy has highly decreased the mortality rate of HNSCC–especially with early-stage diagnosis for patients–many efforts have been made at providing drug-based immunotherapy as an additional form of treatment for the cancer.

Immunotherapy is a common technique used for treatment of diseases afflicting patients, strengthening immune system pathways for fighting diseases by upregulating immune system effector responses as well as with blockers of immune-checkpoint proteins[3]. In the case of HNSCC, which attacks the immune system's responses by mimicking the programmed cell death protein 1 (PD-1) and bypassing immune system security, immunotherapy would address this bypass by the tumor by proliferating another receptor anti-PD-1 (aPD-1) to act as an antagonist, which would inhibit the TNSCC's ability to bind to T-cell by filling the lymphocyte's receptors and allowing for an immune response to properly occur[3]. As detailed in the next section, this experiment primarily involves the observation of aPD-1's effect on tumor kinetics.

B. Primary Objectives

The primary objective of the experiment was to examine the changes in tumor kinetics based on different administered treatments of αPd-1 and radiation therapy. Based on theoretical models and experimental observations, constituting both an experimental and theoretical component to the project as shown in **Fig. 1**. Falling in line with prior publications, the main emphasis of the comparison would be to see how the immunotherapy treatment using the aPD-1 antagonist would affect the tumor's growth over time as well as comparing this newer treatment method to already established methods like radiotherapy of CRT.

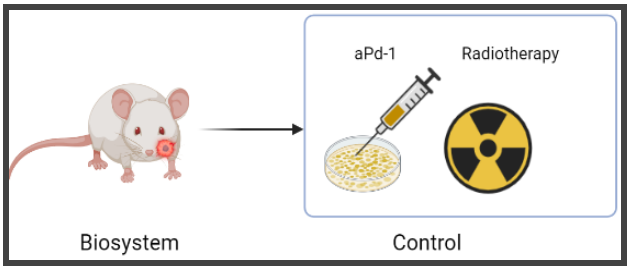

Figure 1. A general illustration of the biosystem and control used for modeling in the project.

Therefore, using these observations as well as knowledge of biosystems and control, another aim for the project was to model the volume profiles of tumor cells based on theoretical calculations and observation with and without control as shown in the simple process block diagram below in **Fig. 2**. The control mouse sample tumor cell volume profile would act as the biosystem alongside the concentration profile of the aPD-1 treatment, with additional control and stability for the system being modeled as radiotherapy was used in conjunction with the immunotherapy.

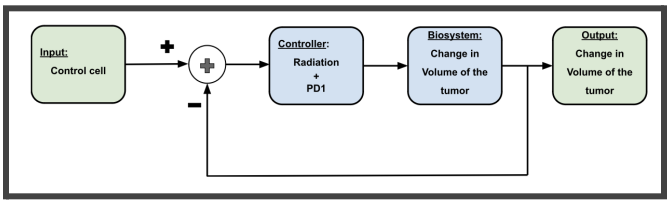

Figure 2. A simple process diagram for the goals of the experiment. The input of the control mouse cell will act as the biosystem for which the immunotherapy treatment and radiation control will be applied. The change in volume of the tumor will be observed and modeled.

Once modeled the next objective was to compare the theoretical and experimental frequency responses for the volume profile and transfer function plots, ideally correlating the stable system with the higher decrease in tumor volume over time (correlating with a better treatment efficacy and positive prognosis for patients).

II. Assumptions

The assumptions for this project are applicable for both the experimental and theoretical aspects. For instance, one assumption was that the mouse sample immune systems were uniform in response, allowing for repeatability with limited deviation in biological factors that would affect the tumor volume. In addition, all treatment controls were assumed to be administered in a uniformed method and rate, allowing for the concentration profile to be modeled. Similarly, the experiment was conducted at standard temperature and pressure with the primary assumption of conservation of mass. Thus, no external stimuli or reaction other than the drug treatment were considered for the volume profile (the radiotherapy was considered as a control later in the experiment). Assuming a constant drug source (syringe) and constant drug sink (tumor cell) allowed for a better conservation model, the variables of which can be found in **Appendix I**. As such, for additional simplification, the mouse model mass, volume, and viscosity were modeled after water and measurement error was neglected for both the theoretical and experimental aspects of the project.

III. Methods

A cancer cell line was cultured within a wet lab within Moores Cancer Research Center at University of California, San Diego. These cells were given to mice, and the subsequent tumors were allowed to develop (**Fig. 3, 4**). Twelve days after the injections, the mice were separated into four sections. The first section had no treatment administered. The second section had only αPd-1 immunotherapy administered. The third section had only radiation administered. The fourth section had a combination of both αPd-1 immunotherapy and radiation therapy administered. Every other day, tumor volume was measured using mechanical calipers and the measurements were recorded. After the tumor sizes plateaued, the mice were sacrificed. The resultant volume data (length and width measurements) were used to determine the volumetric profiles for the experimental portion of the project which were extrapolated from the data gathered.

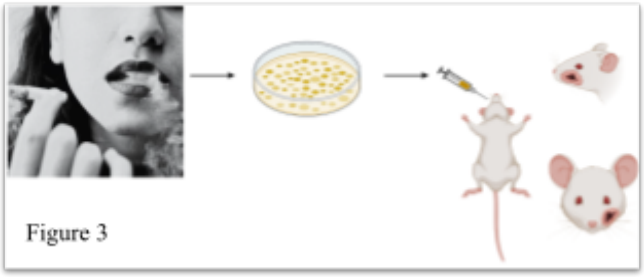

Figure 3. Details the method of injecting cancer cells into mouse specimens before any treatment was administered.

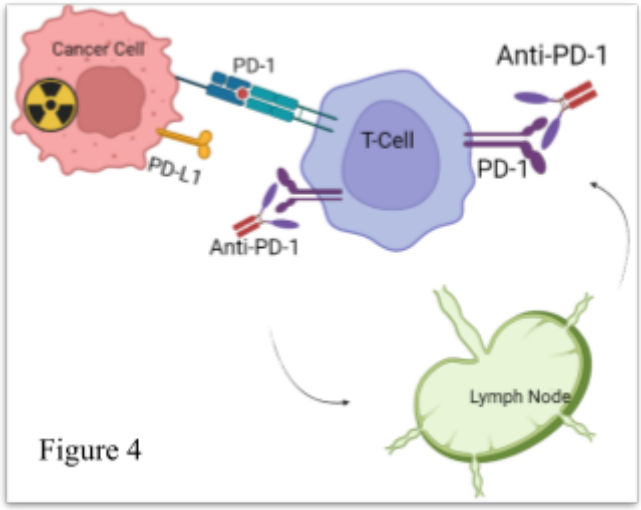

Figure 4. Illustrates the cancer cell mimicking the PD-1 receptors to bind to leukocytic T-cells and prevent an immune response from occurring. The anti-PD-1 drug treatment is also shown acting as an antagonist and filling the receptors before the cancer cells can and allowing an immune response to occur.

For predicting the theoretical kinetics of the tumor volume profile, it was necessary to linearize a set of ODEs based on the concentration profile of the aPD-1 treatment used as well as its interactions between the tumor itself. As shown by **(1)** and **(2)** below, which model the concentration

and volume profiles respectively, the time-invariant system correlates the two profiles together. **Equation (1)** represents the concentration profile for cancer drug treatment aPD-1 with concentration C(t) and drug injection over time I(t), whereas **(2)** represents the mouse tumor cell's volume profile over time based on conservation of mass, including the influx of volume from the concentration of drug treatment being added.

$$\frac{dC}{dt} = \dot{C} = \alpha I(t) - \frac{1}{\tau}C(t) \tag{1}$$

$$\frac{dV}{dt} = \dot{V} = \frac{1}{\tau}V(t) + kC(t)V(t) \tag{2}$$

Since the volume profile needed to be adjusted for small-scale disturbances and linearization, **(1)** and **(2)** were linearized around the operating equilibrium point (C_0, V_0) as defined in **Appendix I**, resulting in **(3)** and **(4)** below. The concentration profile was already linear from the initial system of ODEs and as such remained the same, whereas the concentration profile changed slightly to include that operating point.

$$\frac{d\bar{C}}{dt}_{lin} = \alpha I(t) - \frac{1}{\tau}\bar{C}(t) \tag{3}$$

$$\frac{d\bar{V}}{dt}_{lin} = kV_0\bar{C}(t) + (\frac{1}{\tau} + kC_0)\bar{V} \tag{4}$$

Following this, the now linearized system of ODEs for the concentration and volume profiles were used to solve for the open loop transfer function of the biosystem in terms of volume (V(t)) and drug input rate (I(t)), as shown in **(5)** below.

$$H(s) = \frac{V(s)}{I(s)} = \frac{kV_0\alpha}{(s+\frac{1}{\tau})(s-\frac{1}{\tau}+k*C_0)} = \frac{kV_0\alpha}{(s^2-\frac{1}{\tau^2})} \tag{5}$$

Unfortunately, the biosystem transfer function demonstrated instability due to the positive pole at $\frac{1}{\tau}$, which led to the need for a form of PID control to stabilize the system. In this case, PD control was used to form a stabilized open-loop transfer function for the biosystem and control as shown in **(6)**. Experimentally, the PD control was representative of radiotherapy used in addition to the aPD-1 treatment on the control cells.

$$G(s) = PD * H(s) = \left(s+\frac{1}{\tau}\right)\frac{kV_0\alpha}{\left(s+\frac{1}{\tau}\right)\left(s-\frac{1}{\tau}\right)} = \frac{kV_0\alpha}{\left(s+\frac{1}{\tau}\right)} \tag{6}$$

This new transfer function with a K_d value of 1 and a K_p value of $\frac{1}{\tau}$ allows for the cancellation of the unstable pole via the addition of a zero at the same point, thus allowing for the system to be stable again. Using this, a simple block model was generated using Simulink, as shown in **Fig. 5** below to illustrate the closed loop feedback for the system.

Figure 5: Simulink Block Diagram of aPD-1 Concentration/Volume Profiles

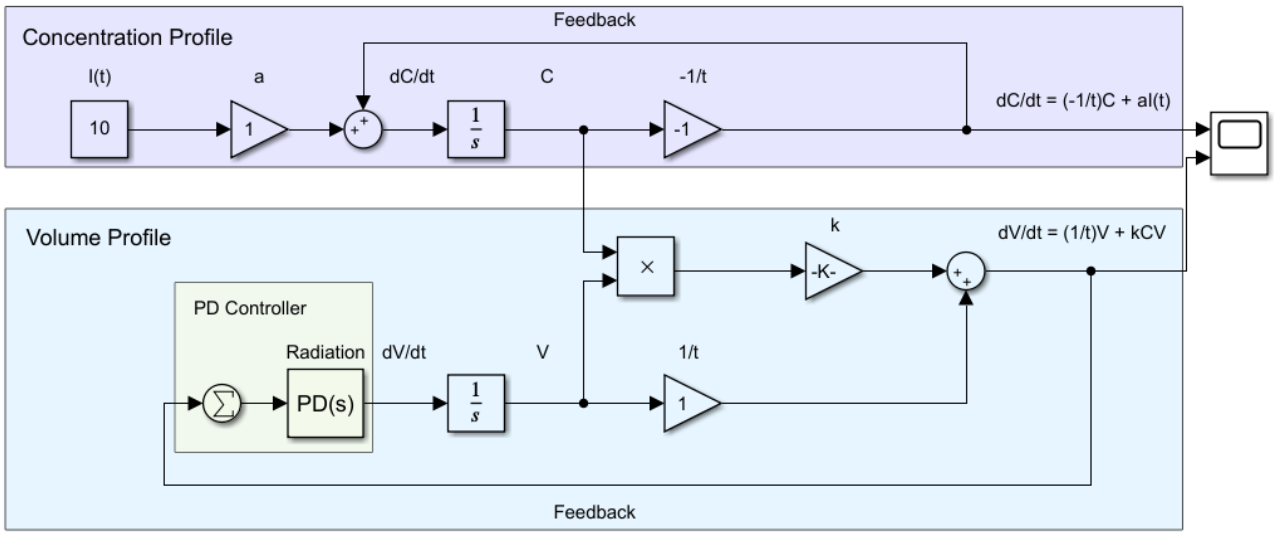

Figure 5. Simple block diagram generated using Simulink to model the closed-loop dynamics and feedback of the concentration and volume profiles for the PD controller and biosystem.

IV. Results

The biosystem (mouse model) was first modeled numerically without immunotherapy and radiation therapy controls. This offered an unstable system which intuitively fell in line with predicted responses given the nature of the cancer and tumorigenesis. As shown in **Fig. 6** below, the unstable response had a non-stable closed loop response with a high negative gain margin.

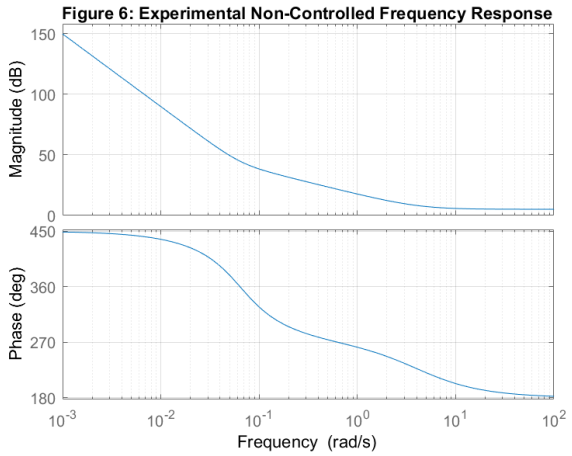

Figure 6. Shows the experimental bode plot of the measured control group without PD-Control. Notice that it is unstable at low frequencies, and critically stable at higher frequency. The system has an unstable gain margin at approximately -5 dB.

On the other hand, applying the radiotherapy and immunotherapy in combination with the experimental biosystem slightly improved the stability of the system extrapolated from the volumetric data, as shown in **Fig. 7**. While not completely closed loop stable due to errors in modeling, the phase margin was in an acceptable range for the system.

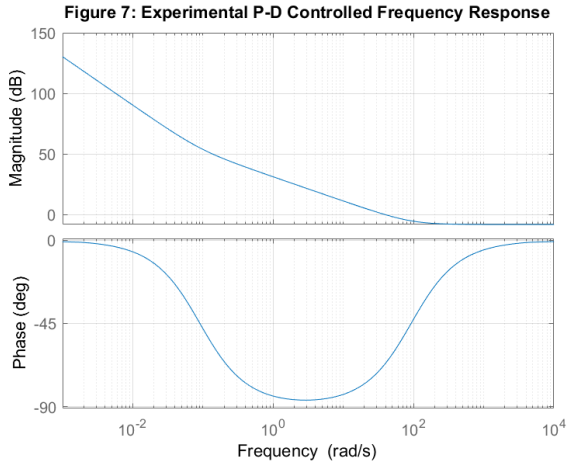

Figure 7. Shows the experimental values of the closed loop system under using the immunotherapy and radiation therapy treatment as control. Notice the stability of the system resulting in high phase margin.

Next, the system was modeled theoretically, both without and with the immunotherapy and radiation therapy controls. In line with the experimental response detailed above, the absence of the radiotherapy control led to an unstable feedback response, whereas the treatment controls were able to push the system into a more stable state as observed in the Bode plot in **Fig. 8**. Modeling the radiotherapy as a PD-controller allowed the system to retain a stable phase margin better than the experimental extrapolation yielded.

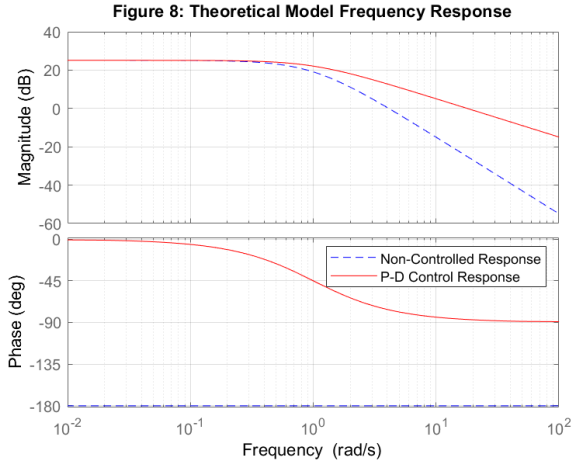

Figure 8. Shows the theoretical bode plots of the system with and without PD control. The dotted blue lines display the unstable closed loop system with no treatment control with an unstable phase margin of 0 degrees. The solid red line shows the stable closed loop system under combination treatment control, with a much more stable phase margin of approximately 90 degrees.

The logical reasoning for the theoretical model as well as the extrapolation of the experimental data was affirmed when observing the cancer volume increasing experimentally, as shown in **Fig. 9**. The varying stability of the control cell samples versus those with different forms of the treatment can be observed in the physical response to the tumors in the mice. The tumors regressed under each form of treatment, with the combined treatment data set proving to have the most effective correlation with tumor volume decrease over the sample time.

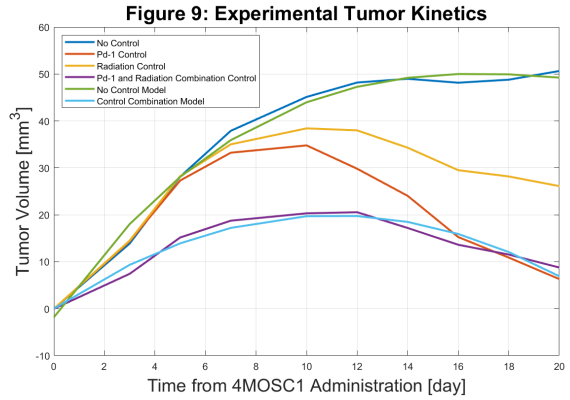

Figure 9. The tumor volume above shows the largest tumors are those without treatment, partial tumor response with immunotherapy and radiation therapy treatments, and near complete response with the combination of treatment. Measurements are taken from the incapacitated mice using mechanical calipers.

V. Discussion

When modeling and simulating the frequency response of the biosystem with and without control, we found that, in general, the addition of control correlated with a more stable system, lining up with predicted results (**Fig. 9**)[3]. In general, each of the treatments, radiotherapy and the aPD-1 immunotherapy, proved to decrease the tumor volume over time as compared to controls, effectively stabilizing the biosystem. Combining the two, however, proved even more effective considering the greater decrease in tumor volume at the end of the sample times (**Fig. 9**).

The HNSCC experimental biosystem and controller were modeled as a closed loop system; however, the models were generated using specific treatments with limited variables. A more robust model that incorporates more variables under increased conditions would be useful to extrapolate data or analyze tumor kinetics. With such, each tumor could be rapidly compared to the system to evaluate the system response to the cancer and treatment. Additionally, there is room for expanding the system to include not only more variables and conditions, but using the same format and concepts for other types of cancer.

A. Disadvantages and Improvements

One of the primary disadvantages to the approach we took with modeling the HNSCC response is that cancer is so diverse and, for the most part, not well understood. Due to the vast complexity of the cancer metabolism and the lymphatic system's response, there are too many variables to effectively model the system response. Thus, the attempts to model a closed system will have little resemblance to reality, and may give rise to misunderstanding or error in an experimental setting, hence the large deviations between the frequency response plots for the experimental models (**Fig. 6, 7**) and the theoretical models (**Fig. 8**). The assumptions taken during the experiment also vastly simplified the processes involved with tumorigenesis, which also affected the gain of the system.

Regardless, there are a number of ways that this experiment and modeling could have been improved to increase the accuracy of the results. For instance, incorporating a delayed measurement error could allow for even more stability with a better phase response for the closed loop feedback, especially since the measurements were done manually with a lower degree of precision. Similarly, incorporating another form of control in addition to the radiotherapy, such as surgical removal, could contribute to an even better response[1]. By improving the model's accuracy, it would be more applicable in clinical and research settings with a lower risk to patients diagnosed with HNSCC.

B. Advantages and Future Application

The advantage to modeling in the above format is the speed at which a biosystem with control can be evaluated in terms of feedback response. The data sets collected for the tumor volume kinetics over time consisted of about 10 volume changes over a span of 20 days, thus allowing for an easy computation based on the model. However, due to the nature of the software available and the transfer function derived for the experiment, we could model much more diverse data sets with similar computational speeds. Additionally, since the data information is already extrapolated, the model can offer an estimate for scientists to compare with future measurements, albeit with less accuracy than other models described in the previous subsection.

Nonetheless, future applications of this modeling design are mostly with the potential of further testing the effects of various treatments on HNSCC or similar cancers in which the tumor kinetics are easily visualized. In the case of which kinetics are unable to be quantified, this model can offer some estimates to follow. Additional models can also be adjusted to demonstrate a more robust cause and effect relationship that will enhance HNSCC treatment on human patients, as well as provide a better direction for future HNSCC research.

Appendix

Appendix I: Theoretical Constants

TABLE I. Theoretical Constants

Transfer Function Constants		
Constant	***Value***	***Units***
α	1	mL^{-1}
τ	1	s^{-1}
k	18	$mg*mL*s^{-1}$
$\mathbf{V_0}$	1	mL
$\mathbf{C_0}$	0	$mg*mL^{-1}$
I(t)	N/A	$mg*s^{-1}$
C(t)	N/A	$mg*mL^{-1}$
V(t)	N/A	mL

Acknowledgment

We would like to thank Professor Gert Cauwenberghs and TAs Becky Chin and Will Sharpless for their time and efforts in assisting us throughout the quarter for BENG 122A's subject material and for offering feedback on our projects and homework.

References

[1] Paleri V, Urbano TG, Mehanna H, Repanos C, Lancaster J, Roques T, Patel M, Sen M. Management of neck metastases in head and neck cancer: United Kingdom National Multidisciplinary Guidelines. J Laryngol Otol. 2016 May;130(S2):S161-S169. doi: 10.1017/S002221511600058X.

[2] Johnson DE, Burtness B, Leemans CR, Lui VWY, Bauman JE, Grandis JR. Head and neck squamous cell carcinoma. Nat Rev Dis Primers. 2020 Nov 26;6(1):92. doi: 10.1038/s41572-020-00224-3.

[3] Pardoll DM. The blockade of immune checkpoints in cancer immunotherapy. Nat Rev Cancer. 2012 Mar 22;12(4):252-64. doi: 10.1038/nrc3239.

[4] Pereira ER, Jones D, Jung K, Padera TP. The lymph node microenvironment and its role in the progression of metastatic cancer. Semin Cell Dev Biol. 2015 Feb;38:98-105. doi: 10.1016/j.semcdb.2015.01.008.

[5] David Chin, Glen M. Boyle, David R. Theile, Peter G. Parsons, William B. Coman, Molecular introduction to head and neck cancer

(HNSCC) carcinogenesis, British Journal of Plastic Surgery, Volume 57, Issue 7, 2004, Pages 595-602, ISSN 0007-1226, doi: 10.1016/j.bjps.2004.06.010.

[6] Saddawi-Konefka R, O'Farrell A, Faraji F, Clubb L, Allevato MM, Jensen SM, Yung BS, Wang Z, Wu VH, Anang NA, Msari RA, Schokrpur S, Pietryga IF, Molinolo AA, Mesirov JP, Simon AB, Fox BA, Bui JD, Sharabi A, Cohen EEW, Califano JA, Gutkind JS. Lymphatic-preserving treatment sequencing with immune checkpoint inhibition unleashes cDC1-dependent antitumor immunity in HNSCC. Nat Commun. 2022 Jul 25;13(1):4298. doi: 10.1038/s41467-022-31941-w.

[7] Wang, Z., Wu, V., Allevato, M., Gilardi, M., He, Y., & Luis Callejas-Valera, J. et al. (2019). Syngeneic animal models of tobacco-associated oral cancer reveal the activity of in situ anti-CTLA-4. Nature Communications, 10(1). doi: 10.1038/s41467-019-13471-0

[8] Zalba S, Contreras-Sandoval AM, Martisova E, Debets R, Smerdou C, Garrido MJ. Quantification of Pharmacokinetic Profiles of PD-1/PD-L1 Antibodies by Validated ELISAs. Pharmaceutics. 2020 Jun 26;12(6):595. doi: 10.3390/pharmaceutics12060595.

[9] Garris CS, Arlauckas SP, Kohler RH, Trefny MP, Garren S, Piot C, Engblom C, Pfirschke C, Siwicki M, Gungabeesoon J, Freeman GJ, Warren SE, Ong S, Browning E, Twitty CG, Pierce RH, Le MH, Algazi AP, Daud AI, Pai SI, Zippelius A, Weissleder R, Pittet MJ. Successful Anti-PD-1 Cancer Immunotherapy Requires T Cell-Dendritic Cell Crosstalk Involving the Cytokines IFN-γ and IL-12. Immunity. 2018 Dec 18;49(6):1148-1161.e7. doi: 10.1016/j.immuni.2018.09.024.

[10] Tranquillo, Joseph Vincent. Biomedical Signals and Systems. Morgan & Claypool, 2014.